An application of operational deflection shapes and spatial filtration for damage detection

Krzysztof Mendrok[*], Jeremi Wójcicki and Tadeusz Uhl

Department of Robotics and Mechatronics, AGH University of Science and Technology
Al. Mickiewicza 30, 30-059, Krakow, Poland

Abstract. In the paper, the authors propose the application of operational deflection shapes (ODS) for the detection of structural changes in technical objects. The ODS matrix is used to formulate the spatial filter that is further used for damage detection as a classical modal filter (Meirovitch and Baruh 1982, Zhang *et al.* 1990). The advantage of the approach lies in the fact that no modal analysis is required, even on the reference spatial filter formulation and other components apart from structural ones can be filtered (e.g. harmonics of rotational velocity). The proposed methodology was tested experimentally on a laboratory stand, a frame-like structure, excited from two sources: an impact hammer, which provided a wide-band excitation of all modes, and an electro-dynamic shaker, which simulated a harmonic component in the output spectra. The damage detection capabilities of the proposed method were tested by changing the structural properties of the model and comparing the results with the original ones. The quantitative assessment of damage was performed by employing a damage index (DI) calculation. Comparison of the output of the ODS filter and the classical modal filter is also presented and analyzed in the paper. The closing section of the paper describes the verification of the method on a real structure – a road viaduct.

Keywords: modal filter; spatial filter; operational deflection shapes; damage detection

1. Introduction

In recent years there has been a significant growth of scientific interest in the local damage detection methods. Authors have mainly focused on high frequency methods, like acoustic emission or guided waves (Klepka *et al.* 2012a, Manka *et al.* 2013, Klepka *et al.* 2012b, Pieczonka *et al.* 2013, Holford 2009). There are also local methods based on substructures analysis. As an example may serve here a work on coupling forces analysis between substructures (Law *et al.* 2010) or method devoted to online substructures identification (Hou *et al.* 2013) This latter method proposes a virtual substructure isolation and identification, with use of time series of measured local responses for online monitoring. However, there are still areas of application where low frequency global methods play an important role. For example, in structures where the critical locations are not known, or in situations when the guided waves cannot be excited. A well-known overview of the latter group of methods can be found in (Doebling *et al.* 1998) and also in (Carden and Fanning 2004). The global methods mainly deal with variation of modal parameters. This is,

---

[*]Corresponding author, Dr., E-mail: mendrok@agh.edu.pl

however, their greatest drawback, because identification of modal parameters is not an autonomous process. The identification of a modal model requires an active experiment with controlled and measured excitation, and this is a further limitation. Of course, there is operational modal analysis where one can identify modal parameters from output-only data, but one obtains not-scaled mode shapes in the results and these cannot be used in various applications. Last but not least, the modal parameters are sensitive to environmental changes. Many of these problems have been solved by the application of a modal filter for damage detection in the manner described in (Deraemaeker and Preumont 2006, Mendrok and Uhl 2010). This approach does not require modal analysis for every diagnosis (only for the reference filter definition) and is said to be robust for environmental changes.

The history of modal filtering began in 1982 with Baruh's and Meriovitch's research, in which filtration was used to overcome the spillover effect while controlling a system with distributed parameters. The problem was that the energy addressed to a particular mode was also delivered to other, uncontrolled, ones, and was solved using a modal filter. Since then, there have been many other successful attempts to introduce this method to a wide range of engineering problems – vibration control of flexible structures, analysis of correlation for experimental and analytical modal vectors, identification of operational forces from the system response and a variety of damage detection and localization methods (Deraemaeker and Preumont 2006, Mendrok and Uhl 2010, Zhang *et al*. 1990, Wentzel 2013, Slater and Shelley 1993, Gawronski and Sawicki 2000, Bahlous *et al*. 2007, Mendrok and Uhl 2008, 2011).

Modal filtration is used to map the modal coordinates of a system from a response vector of a physical space, represented by a network of measurement points, into a modal space. As a result, characteristics describing the dynamic behaviour of single modes can be retrieved. However, there are certain prerequisites that have to be met. First of all, modal analysis, which requires active testing, must be performed in order to reveal the modal coordinates of a system for the reference modal filter formulation. Operational modal analysis is not a solution in this case because one cannot use not-scaled modal vectors to calculate reciprocal modal vectors (modal filter coefficients) according to the original procedure proposed in (Zhang *et al*. 1990). The best results of filtration are obtained using frequency response functions (FRF) data, therefore both input and output must be measured, which makes it very difficult to use modal filtration in operational cases. Such an attempt was successfully conducted in (Mendrok and Kurowski 2013), but the presented algorithm requires a great deal of computational power.

An additional problem is the application of the described method for systems where harmonic components dominate the output spectrum of the system. An example of such a response is presented in Fig. 1.

Modal filters can only filter structural components that possess valid modal coordinates. Harmonic spectral components that are present, e.g., in rotary machines, cannot be filtered using this method and its application requires additional operations (Mendrok *et al*. 2009). Therefore, there is a need to develop a methodology that would overcome these problems and could be used in purely operational cases.

In the paper, the authors formulate and test a methodology for the construction of a spatial filter for ODS that can be applied for filtering of both structural and harmonic components using only system responses. First of all, the theoretical background of ODS is presented and, based on that, the algorithm for ODS filter design is explained. The method is experimentally verified on a small-scale frame model. The model is excited actively by a modal hammer, but a spectral component, treated as a harmonic noise, is also applied by the electro-dynamic shaker. The results

of filtration on the experimental data are discussed and compared with a classical modal filter. Furthermore, the damage detection algorithm that uses the output of ODS filtration is tested on various cases of damage applied to the structure. At the end, the method is applied to the experimental, operational data recorded on the road viaduct. Conclusions are drawn from a detailed investigation of the proposed SHM methodology.

The paper contains following novelties:
- application of an ODS based spatial filter to harmonic components filtration,
- application of an ODS based spatial filter to structural changes detection,
- verification of the method on experimental data,
- verification of the method to operational data recorded on a real technical object.

2. Design of a spatial filter for operational deflection shapes

Spatial filters can be employed for many different applications, but one of the most commonly used is modal filtering. In the classical approach (Zhang *et al.* 1990), construction of such a filter requires a single vector $\{\Psi_r\}$ to be found that will be orthogonal to all modal vectors (consecutive $\{\phi_k\}$ – where $k \neq r$) but not to $\{\phi_r\}$, thus will cancel out the contribution of all modes, except for the *r*-th, providing a function of a single mode only. This approach considers the extraction of only these parts of system response which correspond to individual modes of the system's natural vibration. Design of such a filter requires knowledge of modal coordinates, therefore, this method cannot be applied directly to analyze operational data, where additional components, such as peaks from harmonic vibrations, appear in the response spectra.
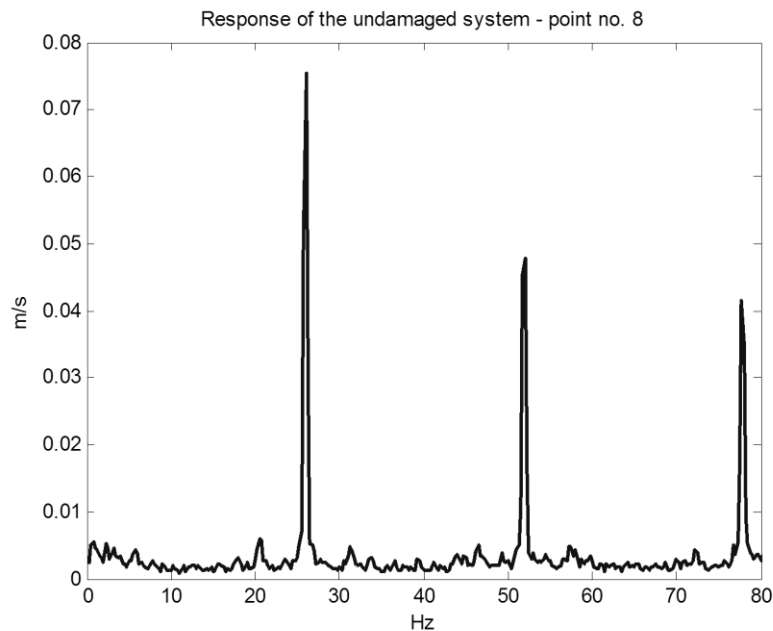

Fig. 1 Example of the response of a system dominated by harmonic components

The ODS filter requires a different approach. It does not operate on FRF and modal vectors, but on responses spectra and ODS. ODS has been defined as the deflection of a structure at a particular frequency or, in other words, ODS can be defined more generally as any forced motion of two or more points on a structure (Schwarz and Richardson 1999). Mode shapes do not possess units and do not carry any information regarding the amplitudes of vibration of the object unless the system's excitation (in terms of amount and location) is known. If identification of the forces exciting the object is too complex or impossible, operational deflection shapes remains the only method that can answer the question of how much the object is actually vibrating (McHargue and Richardson 1993). These features made the ODS a great tool also in the field of damage detection (Zhang *et al*. 2013, Asnaashari and Sinha 2014).

ODS can be obtained from many different types of operational data, both in the time and frequency domain. For the presented method, spectral measurement is of the most interest. For a linear, time-invariant system described with the forced motion Eq. (1), ODS vectors are equal to the response vector *X(jω)* at a fixed frequency.

$$\{X(j\omega)\} = [H(j\omega)] \cdot \{F(j\omega)\} \tag{1}$$

Frequently used data types from which ODS can be retrieved are: linear spectra, power spectral densities (PSD), cross power spectral densities (CSD), FRF and ODS FRF. Modes are strictly related to natural frequencies of the system, on the other hand, ODS can be defined for each frequency from the measuring band, and therefore it is possible to find ODS vectors that will represent spectral components other than modes. In such a case, it would be possible to expand the range of filtration to harmonics and other components of which modal coordinates simply do not exist. That is why the new filtration method would potentially solve the problems mentioned in the previous chapter.

In the method presented here, ODS vectors used for spatial filter design are found by a method of peak picking (Andersen *et al*. 1999), which points to the most dominant peaks in the response spectra. Thus, for such formulation of filtration, modal analysis is not required.

A proper filtering vector needs to fulfil the orthogonality criteria which are expressed by Eq. (2). This means that the filter tuned to extract only the *r*-th signal component, represented by the *r*-th ODS vector $\{\phi_r\}$, is defined by the filtering vector $\{\Psi_r\}$, which must be orthogonal to all selected ODS vectors $\{\phi_k\}$ except for one - $\{\phi_r\}$.

$$\{\phi_k\}^T \{\Psi_r\} = \begin{cases} 1, & r = k \\ 0, & r \neq k \end{cases} \tag{2}$$

The expansion (2) can be expressed as a set of Eq. (3) and solved with respect to $\{\Psi_r\}$ to find a filtering vector for the *r*-th ODS. A more general matrix representation, is presented in Eq. (4), where a set of $\{\rho_r\}$ vectors was replaced with identity matrix.

$$\begin{bmatrix} \{\phi_1\} \\ \vdots \\ \{\phi_n\} \end{bmatrix} \{\Psi_r\} = \{\rho_r\}, \quad \text{where} \quad \{\rho_r\}^T = \{a_1 \dots a_k\} \quad a_i = \begin{cases} 1, & r = k \\ 0, & r \neq k \end{cases} \tag{3}$$

Usually in SHM systems, large arrays of sensors are used and only a limited band with a few

modes is considered. Therefore, the system of equations created is under-determined, that is, there are more unknowns than equations. As a result, the ODS matrix is not square, so not invertible, therefore pseudo inversion is proposed in order to find a proper solution of the linear set of Eq. (3), similarly to the approach described in (Zhang *et al.* 1990).

$$\{\Psi\} = \{\phi\}^{+} \cdot [I] \tag{4}$$

where: *[I]* is the identity matrix equal in size to the number of ODS vectors, and $^{+}$ is pseudoinverse.

Filter output is calculated as a dot product of the filtering vector $\{\Psi_r\}$ and ODS vectors of system responses at each frequency in the whole band (5). Filter output is denoted as $\eta(\omega)$ and $p_i(\omega)$ is the PSD of response spectra of the *i*-th measurement point.

$$\eta(\omega) = \{\Psi_r\}^{T} \cdot \begin{bmatrix} \{p_1(\omega)\}^{T} \\ \vdots \\ \{p_n(\omega)\}^{T} \end{bmatrix} \tag{5}$$
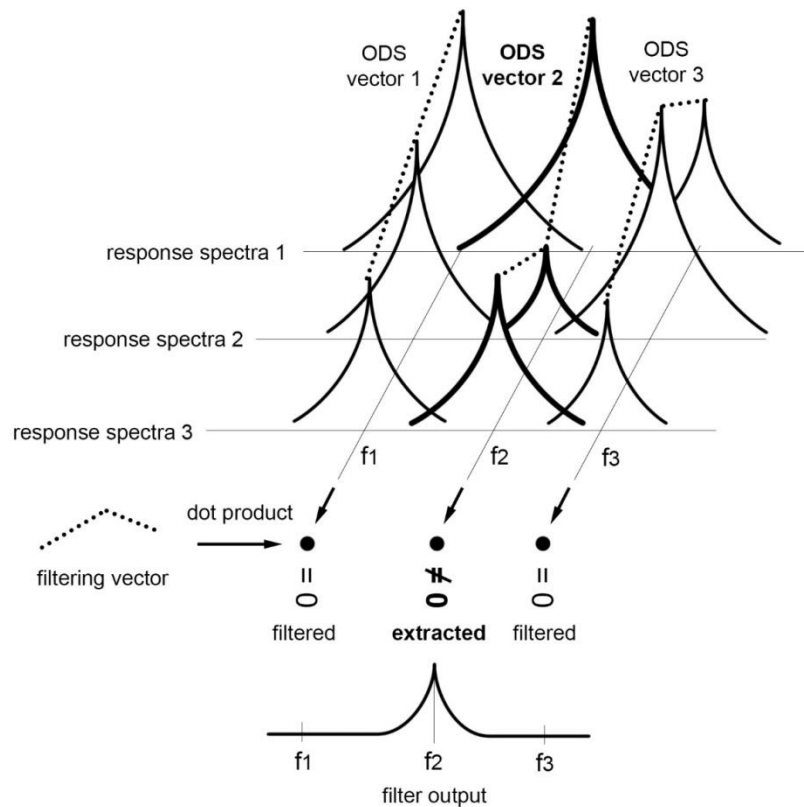

Fig. 2 Graphical presentation of spatial filtration for the ODS principle

Fig. 2 graphically presents the principle of ODS component filtering. Each component is represented by a single ODS vector which is located at its maxima. The main assumption is that ODS vectors contributing to the same component are linearly dependent. The filtering vector which is perpendicular to the ODS vector at its peak is also perpendicular to every other vector of that component, and will be able to cancel out its whole contribution to response spectra.

In the case of structural changes in the tested object, imperfectly filtered peaks occur in the spectra, which lay a basis for damage detection. For the purpose of evaluation and tracking of structural changes in the object, the damage assessment algorithm proposed in (Mendrok and Uhl 2010) can be utilized (6). Calculation of the damage index (further denoted as DI) is conducted by estimating the relative change in the area of the filter output using bandwidth in the direct neighbourhood of the analyzed frequency. Imperfectly filtered peaks occurring in the filter spectra contribute to the total, averaged DI of the system.

$$DI = \frac{\int_{\omega_s}^{\omega_f} \left| x_i(\omega) - x_{ref}(\omega) \right|^2 d\omega}{\int_{\omega_s}^{\omega_f} x_{ref}(\omega)^2 d\omega}$$

(6)

where: ω_s – starting frequency of the analyzed band,
$\quad\quad \omega_f$ – closing frequency of the analyzed band
$\quad\quad x_i$ – characteristic in the current state
$\quad\quad x_{ref}$ – characteristic in the reference state

The procedure for the ODS filter design has been summarized in the flowchart presented in Fig. 2. The algorithm consists of two main phases: the filter design, in which the coefficients of the filter are estimated, and construction of the SHM system with a capability for damage detection using the prepared ODS filter.

3. Experimental verification

Simulation verification of the method confirmed its usefulness in the filtering of ODS components (Wojcicki *et al.* 2013). Therefore, there is a justified need to test the proposed algorithm in real-life conditions, such as an experiment in a controlled environment should provide. In the test, damage to the structure under scope is represented by adding various weights in several locations on the object, which will change its dynamic behaviour. The desired outcome of the test is to identify whether such damage occurred and assess its magnitude. Additionally, an unmeasured harmonic excitation will be applied to the object, in order to check whether the method can successfully extract or filter out the harmonic components present i.e., in rotary machines, such as power generator, electric motors and gearbox systems etc.

Measurements are always affected by some external, unmeasurable factors (such as electrical noise, non-linearity of the examined system or other unpredicted sources of vibration), as a consequence the results of each test differ. Therefore, robustness of the method is also going to be evaluated by assessment of the influence of the mentioned disturbances on the results in the measurement runs with the same setup.

3.1 Test setup

The object of the test is a metal frame consisting of three aluminum beams, two of which are attached to the steel base of significant weight, preventing the displacement of the whole structure with respect to the ground. A photograph of the tested frame is presented in the right hand side of Fig. 3, its scheme with measuring points, excitation locations and added masses is presented in the left hand side of the figure. Seven accelerometer sensors were located at the central beam. Points 1 and 2 are the places where additional weights are mounted. "Ex" denotes an excitation point at which wide band excitation is applied to the frame using an impact hammer. Point "S" denotes the place where a harmonic type of excitation is supplied with a shaker at the frequency of 150 Hz.

The measurements were carried out using LMS SCADAS III and seven single axis ICP accelerometers (PCB 333B31). For the excitation of the structure, a PCB 086C03 impact hammer and SmartShaker K2007E01 were used. The bandwidth of the acquisition was 1024 Hz, with a frequency resolution of 0.5 Hz. Hamming windows were utilized and each measurement consisted of five averages. The PSD of each channel's responses was calculated and used for the formulation of the ODS matrix.

3.2 Results of the experiment

In Fig. 4, the summation function of the PSD of system responses was presented. There are four dominant peaks at frequencies of 66 Hz, 121 Hz, 150 Hz and 224.5 Hz. ODS vectors for these frequencies will be used as an input for calculation of ODS filter coefficients.

In Fig. 5, ODS of the structure are presented. Shapes 1, 2 and 4 are mode shapes related to the first three natural frequencies of the object (66 Hz, 121 Hz and 224.5 Hz). Except for wide-band excitation with an impact hammer, the structure was additionally excited with a sine signal of fixed frequency and amplitude at 150Hz applied by the shaker, which resulted in ODS 3. This is a combination of neighbouring mode shapes, each of them having a partial contribution to the final shape of ODS 3. The places in which the additional weights P1 and P2 were attached are marked with thin black lines.

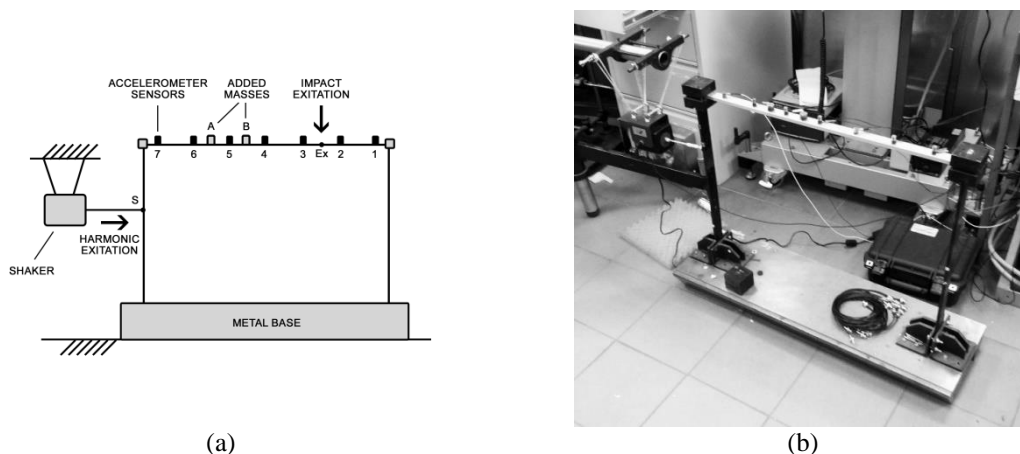(a)   (b)

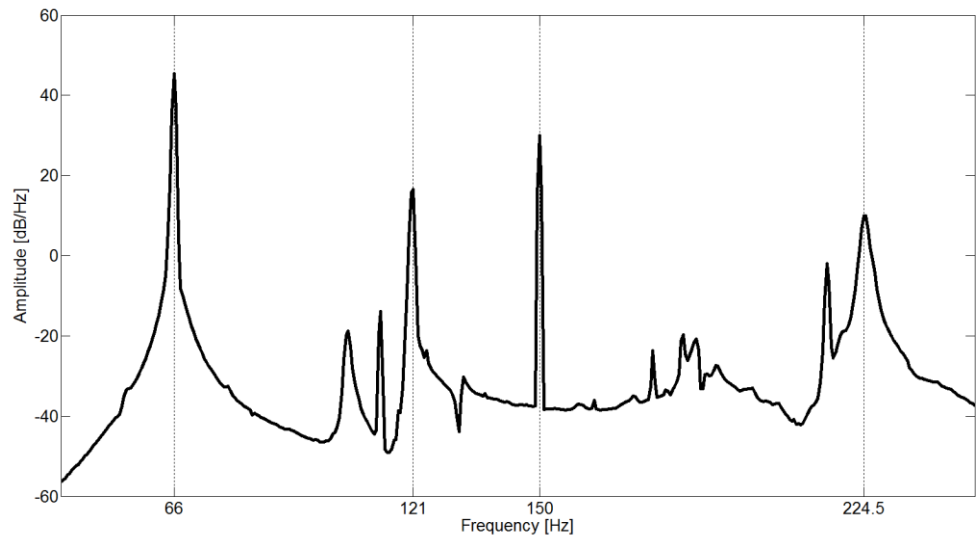Fig. 3 Schematic (a) and picture (b) of the setup for the experiment
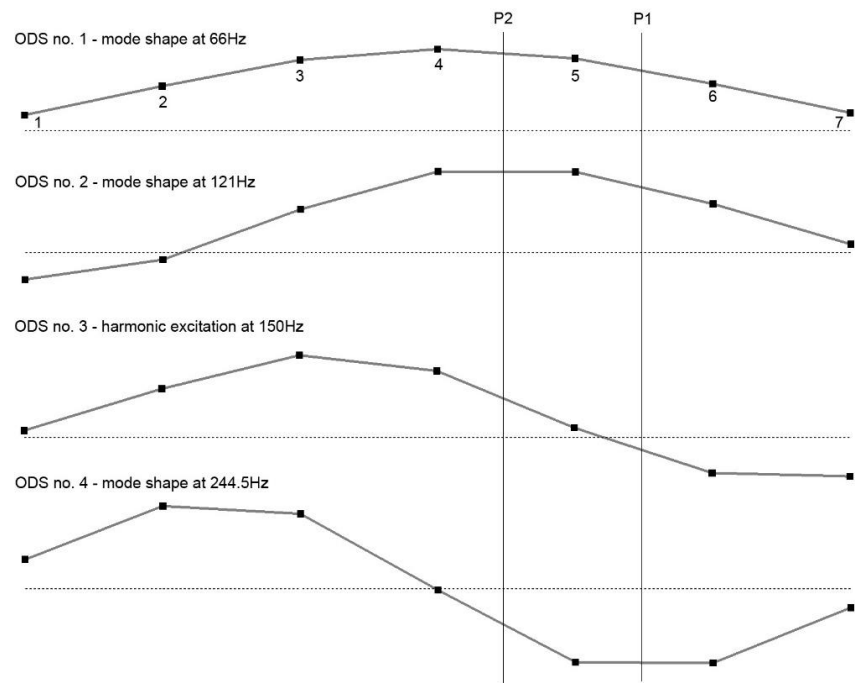
Fig. 4 SUM indicator of system output

Fig. 5 Visualization of deflection shapes for selected components

3.2 Results of the experiment

In Fig. 4, the summation function of the PSD of system responses was presented. There are four dominant peaks at frequencies of 66Hz, 121Hz, 150Hz and 224.5Hz. ODS vectors for these frequencies will be used as an input for calculation of ODS filter coefficients.

In Fig. 5, ODS of the structure are presented. Shapes 1, 2 and 4 are mode shapes related to the first three natural frequencies of the object (66 Hz, 121 Hz and 224.5 Hz). Except for wide-band excitation with an impact hammer, the structure was additionally excited with a sine signal of fixed frequency and amplitude at 150Hz applied by the shaker, which resulted in ODS 3. This is a combination of neighbouring mode shapes, each of them having a partial contribution to the final shape of ODS 3. The places in which the additional weights P1 and P2 were attached are marked with thin black lines.

3.3 Results of filtration on experimental data

In Fig. 6, the output of filtration is presented, with each filter on a separate graph. Two cases are considered: the first one, "no damage" case, is an initial test, the results of which were used for the estimation of the filter coefficients, and the second one, "no damage ref", is a referential measurement for which the designed filter was applied. The similarity between results is high and, in both cases, it can be observed that the method properly extracted peaks at the frequencies to which the filter was tuned. The most representative filtration results were obtained for Filters 1 (66 Hz) and 3 (150 Hz), whereas in the remaining two filters some imperfections are visible. In the "no damage" case, the amplitude of filtered components reach exactly the value of 1, meeting mathematical criteria specified in Eq. (2), however, some small distortions can be observed in the referential test as peaks reach values slightly larger than one.
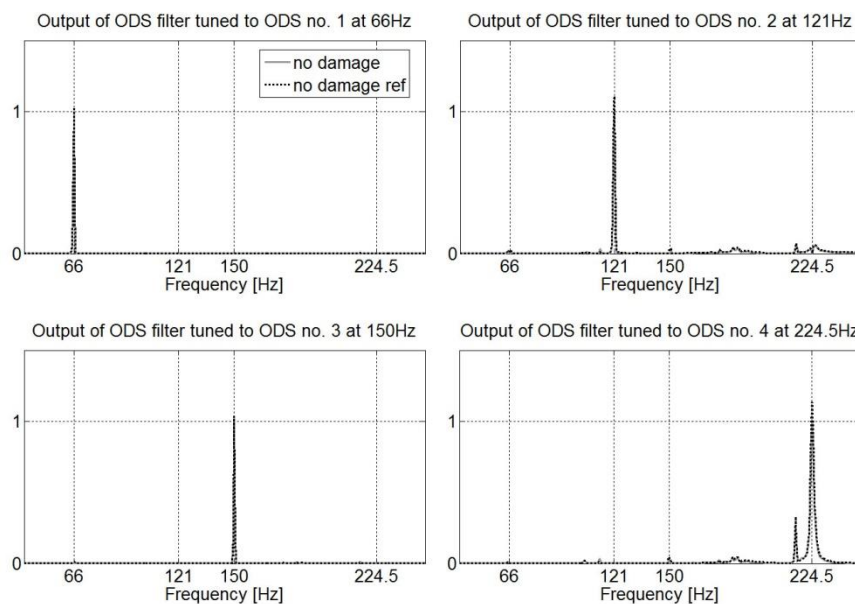

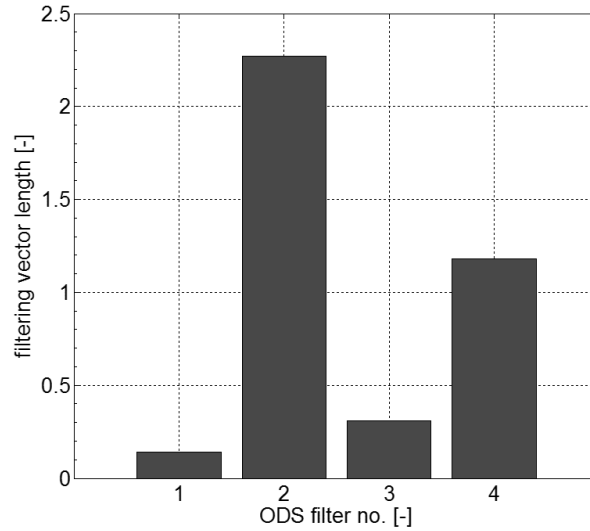Fig. 6 Output of the ODS filters for non-damage cases

Fig. 7 Lengths of the filtering vectors for ODS Filters 1-4

To explain why some of the filters worked better than the others, one must consider the influence of a particular filtering vector on the output. The dot product of the ODS vector ϕ_r to which the filter was tuned and the filtering vector Ψ_r is equal to one, which was, using the definition of the dot product, expressed in Eq. (4). The conclusion that arises from the equation is that the length (module) of the Ψ_r vector depends on two factors: the length of ϕ_r and the angle θ. When the expression in the denominator of Formula (4) approaches zero (meaning that the shorter ϕ_r and the closer to 90° θ angle are the longer Ψ_r vector is). The length of the consecutive vectors is presented in Fig. 7. But how does the length of the Ψ_r vector affect the quality of filtration? Only four ODS vectors were chosen to build the filter, but many more peaks can be observed in the SUM indicator (Fig. 4). These peaks are not filtered out, as they were not included in the estimation of filter coefficients. The amplitude of these peaks in the filter output mostly depends on the considered module of the filtering vector, as they also undergo the dot product calculation. If the length of Ψ_r is kept low, the amplitude of unwanted peaks is also low, if high, on the contrary - they are amplified. To overcome the problem, only the most dominant peaks shall be chosen for the filter design. Also if the ODS and filtering vector happen to be close to parallel (according to Eq. (7)), it will decrease the length of Ψ_r providing the best possible filtration quality.

$$\left|\Psi_r\right| = \frac{1}{\left|\phi_r\right| \cdot \cos\theta}$$

(7)

3.4 Damage detection test

The damage detection algorithm consists of three phases. In the first phase, the output of filtration is captured, yielding a function in the frequency domain, as in Fig. 6. For the structure

under investigation, four active filters have been applied, tuned for each ODS vector, which gives a more comprehensive insight into the object behaviour.

Phase 2 is a calculation of the damage index, as described earlier in the paper, according to which a single value, representing structural change in the structure, is obtained by each filter. The damage index provides information about relative changes of the spatial filter output with respect to the reference state. For its calculation, a 10% bandwidth around the considered frequencies was established. It is important to understand that it is not frequency drift that is being captured by the algorithm, but the change in the deflection shape, resulting in alternation of the ODS vector. This change causes a shift in the angle between the ODS itself and the filtering vector. As was stated before, in the reference state of the object, the filtering vector was perpendicular to all the ODS, except one (to which the filter was tuned), so the dot product was equal to zero, but after alternation, this criteria will no longer be fulfilled. As a result, additional peaks show up in the filter spectra, the appearance of which is indicated by the damage index.
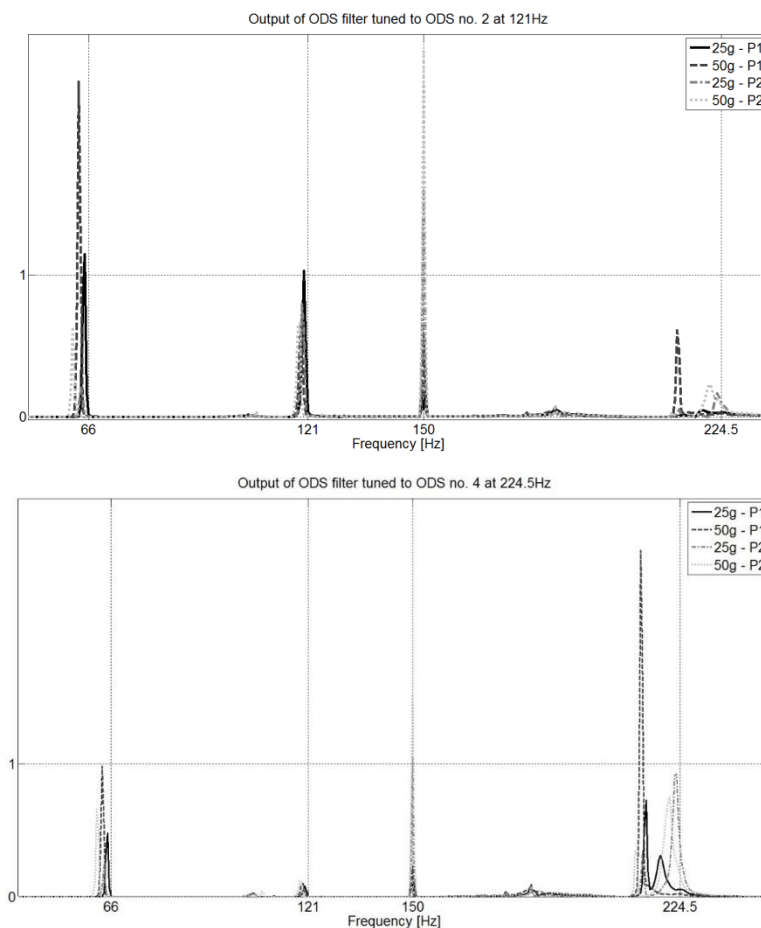

Fig. 8 Output of ODS Filters 2 (121 Hz) and 4 (224.5 Hz) with a mass of 25 or 50 g added to points P1 and P2
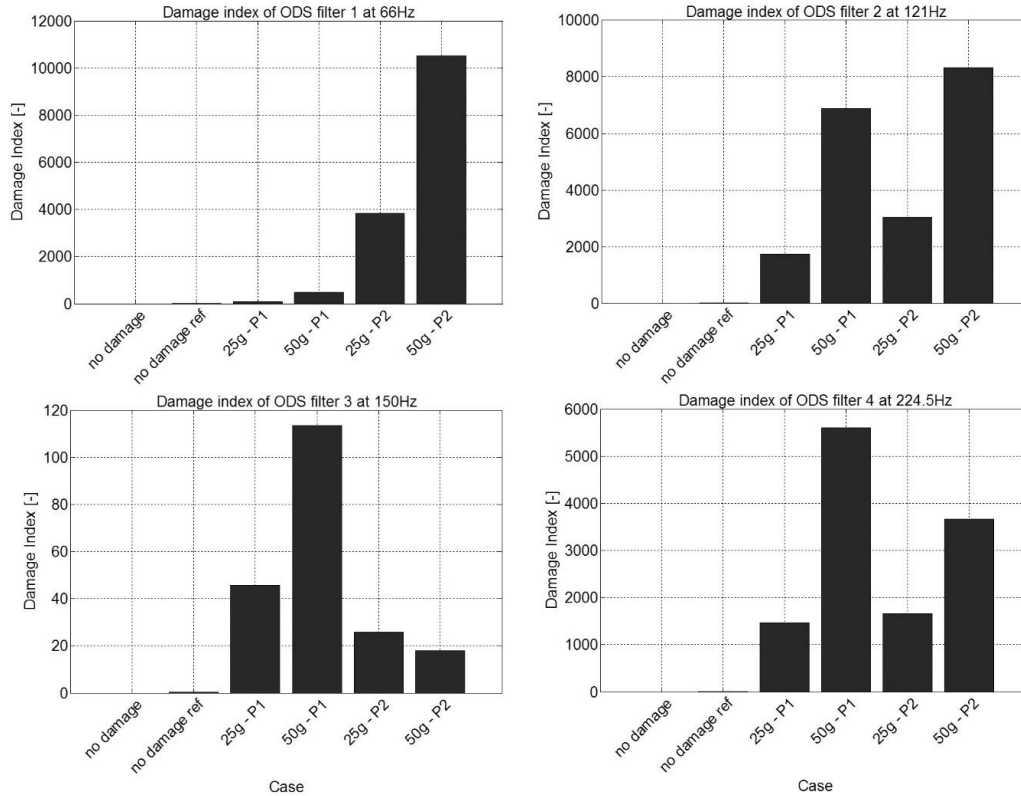
Fig. 9 Damage Index calculated from ODS filters output for every case of damage considered

In the final phase, the average of all the DI values is calculated. This indicator can be interpreted directly, by comparing with the DI for the object in reference state, or can become an input for another algorithm, such as neural network, fuzzy logic etc. in the SHM system. The final indicator can successfully be used to track propagation of the damage because, as will later be demonstrated, it carries information about the magnitude of structural change.

The results of filtration with four different cases of damage applied to the structure are presented in Fig. 8. Filters 2 and 4 were chosen, as their outcomes were the most representative. The level of DI for each of the filters for every considered case is presented in Fig. 9. The results are consistent – the higher the amount of mass attached, translating into "bigger" damage to the structure, the higher the indicator. The only exception is Filter 3, the "P2" case, in which the damage detected for a higher mass of 50 grams is lower than for 25 grams. An explanation of this phenomenon can be found in Fig. 8. It seems that the higher amount of mass created a higher damping factor for that mode, so during the integration process for the DI calculation, the area enclosed under this peak was smaller and resulted in a lower DI.

In Fig. 10, an averaged damage index for each case is presented. Most importantly, it can be spotted that the DI for "no damage ref" of 3.35 is very low in comparison with other cases (lowest is "25g – P1" of 832), in which structural change was applied to the object under investigation. This regularity can also be spotted in DI charts for each of the filters. Such a huge difference

between the damaged and undamaged beams proves that the method does not return false-positive. For the purpose of an SHM system based on ODS filtration, the alert threshold could be safely set to 10-20 times the DI in the reference test.

Another conclusion drawn from the results is that the method is also magnitude sensitive – the more damage applied, the higher the damage index obtained. Doubling the mass (from 24.5 to 49 grams) for cases "P1" and "P2" made the DI almost 4 and 2.5 times higher, respectively.

Although the same amount of mass was attached to the structure in points "P1" and "P2", the assessed damage is considerably higher for the second case. An explanation of this is simple. It is a well-known fact that the structural change in the object will affect a particular mode or, in this case, ODS mostly if the location of the damage is close to the antinode of the shape, and least if it is close to a node. Table 1 gathers information regarding the closeness of points "P1" and "P2" to the nearest peak or node. It is clear that the location of "P1" is generally closer to nodes of the considered ODS, and "P2" is more often located near the antinode, therefore the method showed greater sensitivity for the damage located at this particular point. The matter of selecting a proper set of ODS is of critical importance – if one chooses a set of ODS that all have a node in the same location, potential damage that could occur at that spot might not be detected, as it will weakly influence the shape and might be omitted by the filter.
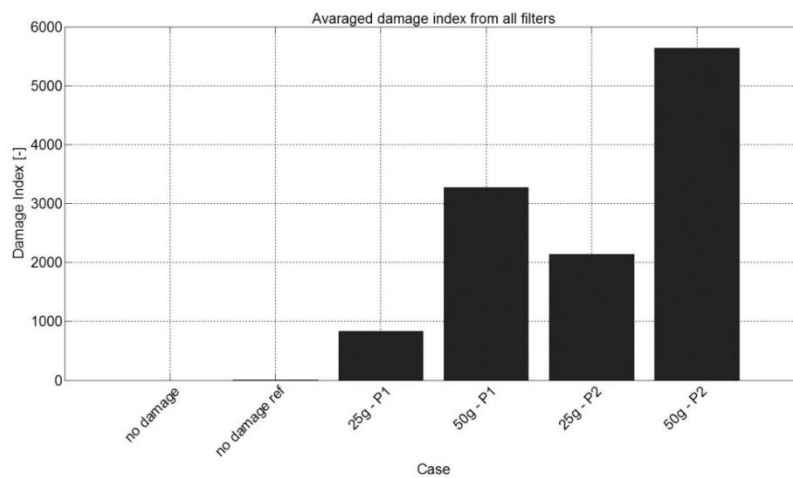

Fig. 10 Averaged damage index calculated for every damage case under scope

Table 1 Location of damage points for each ODS

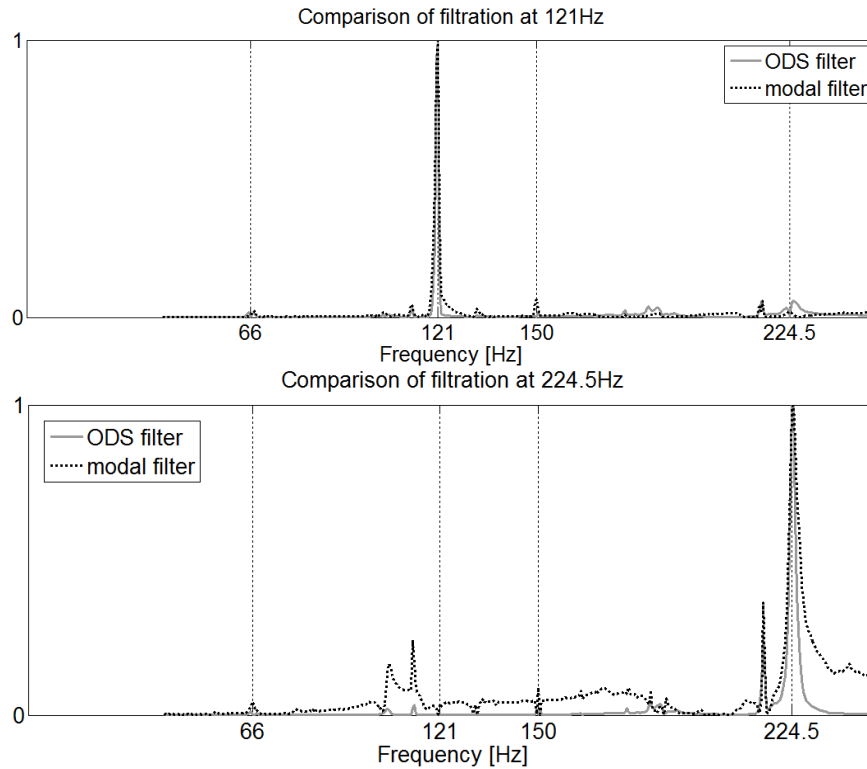| ODS no.	P1	P2
1	closer to node	closer to antinode
2	closer to node	closer to antinode
3	close to node	close to node
4	closer to antinode	closer to node

Fig. 11 Comparison of ODS and modal filter. The figure presents the output of different filters tuned to the frequency 121 Hz (the upper graph) and to 224.5 Hz (the lower graph)

3.5 Comparison of ODS filter and classical modal filter

The output of the ODS filter was compared with the output of the classical modal filter. The modal filter was applied on a different type of data - frequency response functions measured between the input from the impact hammer (which was measured for this test) and output from the response points on the structure. Modal filter design required knowledge of modal coordinates of the system, therefore modal analysis was performed. The results of the comparison are presented in Fig. 11. For the purpose of comparison, the output of the modal filter was normalized to 1.

In the 121 Hz case, corresponding to the filtration of the 1st mode and 1st ODS vector, the convergence of the graphs is high and both filters properly extracted the desired mode/ODS. Some noise can be observed in the remaining band for both filters, however the modal one showed worse results with the filtration of 150 Hz harmonic components. A larger difference can be spotted for the second case (224.5 Hz), corresponding to the 3rd mode and the 4th ODS vector. In this case, ODS filter is virtually noiseless when compared to classical modal filter, and very few imperfections are present in the output. The modal filter did not work well in this case, as many imperfectly filtered peaks distort the spectra. The harmonic component was not handled well by the filter, which can be explained by the fact that this type of method is capable of filtering only modal components.

4. Spatial filter formulation for the road viaduct data

The object of the analysis was the five-span road viaduct over local street in Bochnia. The object is a part of the international road E40 between Krakow and Tarnow. The volume of traffic on this road is very high. The tested viaduct consists of five spans of length of 18.94 + 19.53 + 19.62 + 19.61 + 18.70 = 96.40 m. Its total width amounts 11.40 m: the roadway - 7.00, and the shoulders - two times 2.00 m. The picture of the viaduct under investigation is shown in Fig. 12b.

The static scheme of the viaduct is the frame of five-spans. The main supporting structure is made from prefabricated pre-stressed 18.00 m long beams. Over the supports the beams are joint together and connected with the pillar branches to behave like perpetual ones. There exist 8 beams with 1.5 m axial spacing in the crosswise section. With the beams - girders mates the reinforced concrete plate of the viaduct deck of thickness of 12 - 18 cm.

The bridge heads are supported on two pillars, and each of the middle supports consists of one pillar. All the pillars have foundations made from reinforced concrete piles. The fittings elements are typical for the road viaducts.

4.1 Modal experiment

The modal experiment on the described viaduct was performed. During the test operational excitation was used, that is the traffic on the viaduct deck, wind and soil vibrations (Uhl *et al*. 2001). The measuring points net consist of 42 points and was divided into three components:
- 18 points spaced along the most left girder of the viaduct,
- 18 points spaced along the most right girder of the viaduct,
- 6 points spaced along the forth girder from the right on the middle span.

The measuring point net is presented in Fig. 12(a).

The sensors were mounted to the bottom surface of the girders. Because of the height of the object there were two climbers and the truck with jib employed for the purpose of the sensors placement.

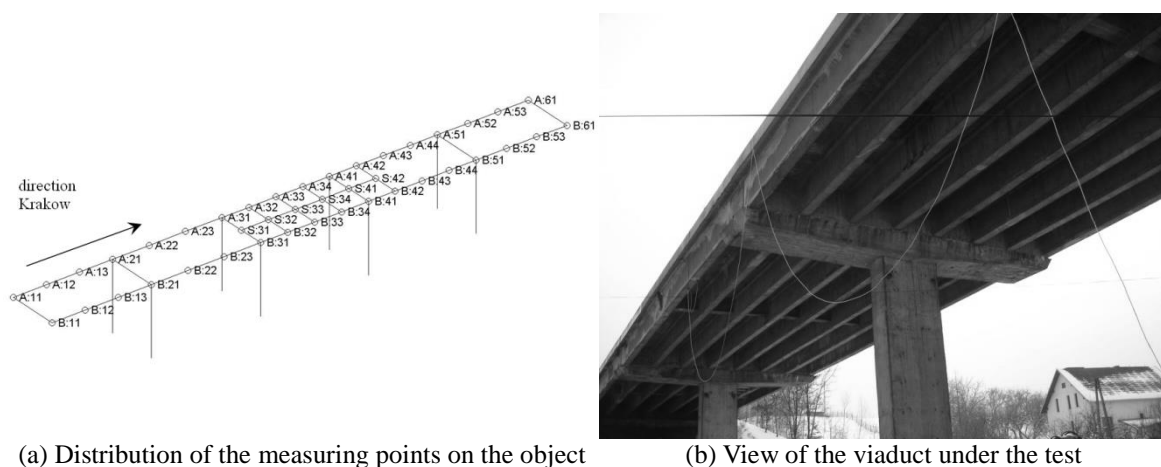(a) Distribution of the measuring points on the object   (b) View of the viaduct under the test

Fig. 12 Object of investigation

The 900-second time histories of the vibrations acceleration were recorded with 100 Hz sampling frequency. The long period of acquisition is required in such a measurements, to provide possibly unique excitation conditions in each partial experiment, and to achieve high frequency resolution in further analysis. However, authors were limited here, because the experiment could not last more than one day. In every of the five partial experiments 9 response and 1 reference points were measured. For the data acquisition the digital recorder TEAC GX-1 with 16 channels and 10 seismic accelerometers PCB 393A03 were used.

4.2 Modal analysis

The modal parameters estimation was predated by the analysis of the stored data quality. The spectra from the reference point for each of the partial experiments were compared. Their similarity indicates, that the level of excitation was appropriate in each of the tests. The modal parameter estimation was carried out with use of the MDOF module of the modal analysis software package VIOMA (Uhl *et al.* 2001). LSCE and BR estimation algorithms were applied. The set of estimation procedures was performed, and from its results the most representative mode shapes were selected with use of the original procedure for the modal model consolidation Lisowski (2003).

At first the modal analysis of entire object was performed. The results of modal parameter estimation are listed in Table 2. Plots of some of the identified mode shapes are presented in Fig. 13. The modes are well separated and excited during the experiment. Tested bridge is relatively stiff structure, but some of the identified global mode shapes indicate, that the stiffness of particular girders is different. There are some local modes, recognized in identification results, which are localized on the left side of the viaduct. The modal damping coefficients have relatively high value in comparison with results obtained for similar objects.

Table 2 Results of modal parameter estimation

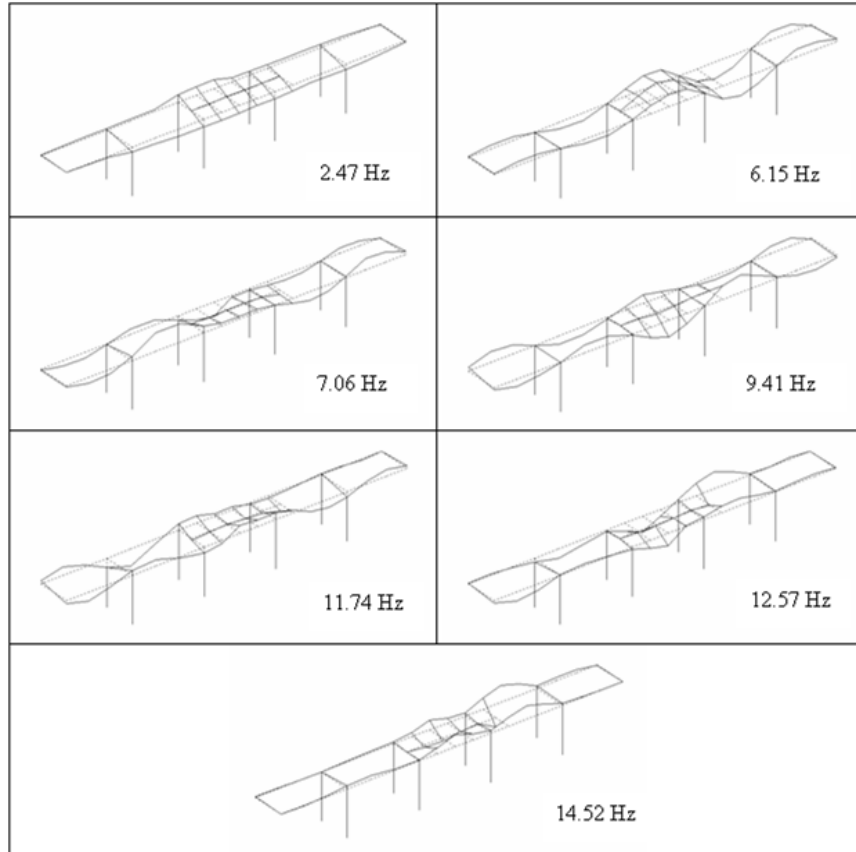| MS no.	Natural frequency [Hz]	Damping coeff. [%]
1	2.47	4.65
2	6.15	2.64
3	7.06	3.18
4	9.41	2.46
5	11.74	2.96
6	12.57	1.41
7	13.37	1.45
8	14.52	1.91
9	15.48	0.29

Fig. 13 Mode shapes of the tested viaduct

4.3 Spatial filter formulation

To check the applicability of the proposed method for real technical objects, the spatial filter was formulated for the data gathered in the described experiment. The same SUM index was used for ODS determination as for the operational modal analysis. To increase accuracy of the spatial filter, a larger number of ODS was selected than the number of identified mode shapes. The SUM index with peaks for which ODS were determined and marked with circles is presented in Fig. 14.

23 ODS were formulated and, on their basis, appropriate spatial filters were calculated. The results of filtration with use of these filters can be observed in Fig. 15. The filtration of other components than the one to which the spatial filter was tuned is not perfect but, in the opinion of the authors, it is sufficient to apply it for damage detection. The problems with filtration of some components from the system response, although 23 ODS were used for filter formulation, seem to indicate that there is no need for so many ODS formulations, as similar results were obtained for the number of ODS consistent with the number of mode shapes. Despite these problems, the obtained results are promising and show prospects for the application of ODS based spatial filters in the monitoring systems of technical structures.
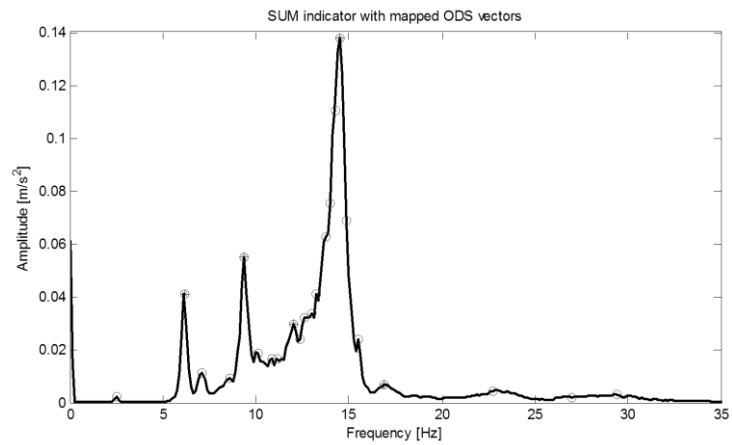
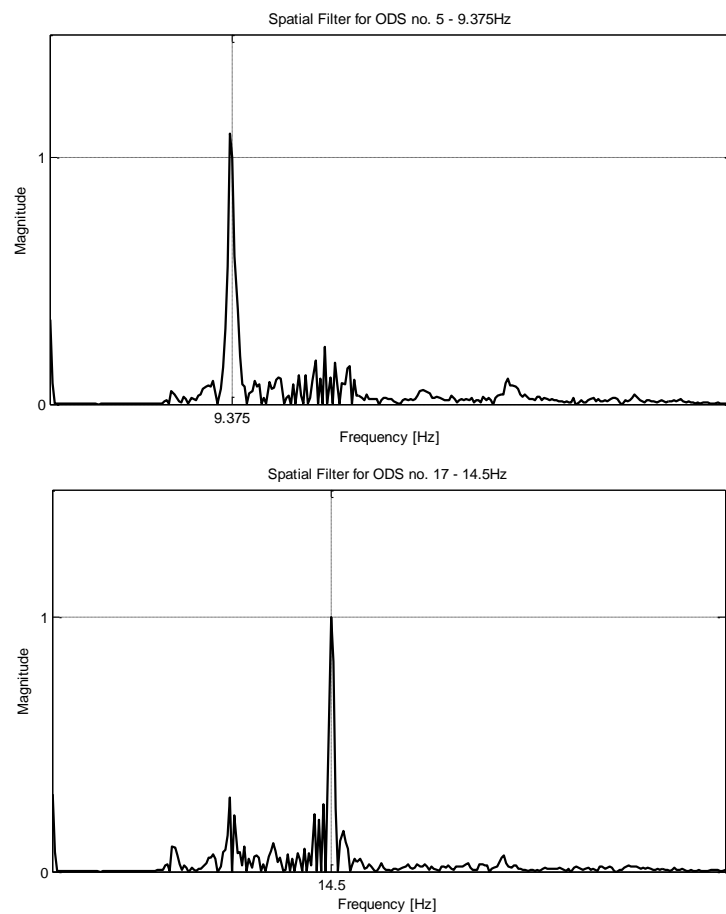Fig. 14 SUM indicator with marked ODS

Fig. 15 Example of outputs of spatial filter for the viaduct data

5. Conclusions

Filtering ODS using a spatial filter has been widely discussed in this article and proved to work on the case study example. A method for filter construction by relatively simple mathematical means and with no knowledge of modal coordinates of the system was presented. Quality as well as imperfections in filtration output were considered and explained according to the proposed quality indicator. The proposed damage detection algorithm was implemented using obtained operational data and several cases, with structural changes applied to the object, were analyzed. Damage, its presence and magnitude, was successfully identified, based on the change in deflection shapes of the structure, using the considered filtration method. The method allowed not only the filtering of spectral components related to mode shapes (as in a similar approach – modal filter), but also harmonic components, applied from external, unmeasurable sources. Comparison with the classical modal filter revealed a few advantages of the ODS filter when used in operational conditions. Overall, the test results are satisfactory and the method seems to be stable and reliable for SHM purposes.

Acknowledgments

References

Andersen, P., Brincker, R., Peeters, B., De Roeck, G., Hermans, L. and Krämer, C. (1999), "Comparison of system identification methods using ambient bridge test data", *Proceedings of the 17th International Modal Analysis Conference,* Kissimee FL, February.

Asnaashari E. and Sinha J.K. (2014), "Development of residual operational deflection shape for crack detection in structures", *Mech. Syst. Signal Pr.*, **3**(1-2), 113-123

Bahlous, S.E.O., Abdelghani, M., Smaoui, H. and El-Borgi, S. (2007), "A modal filtering and statistical approach for damage detection and diagnosis in structures using ambient vibrations measurements", *J. Vib. Control*, **13**(3), 281-308.

Carden, E.P. and Fanning, P. (2004), "Vibration based condition monitoring: a review", *Struct. Health Monit.*, **3**(4), 355-377.

Deraemaeker, A. and Preumont, A. (2006), "Vibration based damage detection using large array sensors and spatial filters", *Mech. Syst. Signal Pr.*, **20**(7), 1615-1630.

Doebling, S.W., Farrar, C.R. and Prime, M.B. (1998), "A summary review of vibration-based damage identification methods", *Shock Vib. Dig.*, **30**(2), 91-105.

Gawronski, W. and Sawicki, J.T. (2000), "Structural damage detection using modal norms", *J. Sound Vib.*, **229**(1), 194-198.

Holford, K.M. (2009), "Acoustic emission in structural health monitoring", *Key Eng. Mater.*, **413**, 15-28.

Hou, J., Jankowski, Ł. and Ou, J. (2011), "A substructure isolation method for local structural health monitoring", *Struct. Control Health Monit.*, **18**, 601-618.

Hou, J., Jankowski, Ł. and Ou, J. (2013), "An online substructure identification method for local structural health monitoring", *Smart Mater. Struct.*, **22**(9), art. no. 095017.

Klepka, A., Staszewski, W.J., Jenal, R.B., Szwedo, M., Iwaniec, J. and Uhl, T. (2012a), "Nonlinear acoustics for fatigue crack detection–experimental investigations of vibro-acoustic wave modulations", *Struct.*

Health Monit., **11**(2), 197-211.

Klepka, A., Staszewski, W.J., Uhl, T., Di Maio, D., Scarpa, F. and Tee, K.F. (2012b), "Impact damage detection in composite chiral sandwich panels", *Key Eng. Mater.*, **518**, 160-167.

Law, S.S., Zhang, K. and Duan, Z.D. (2010), "Structural damage detection from coupling forces between substructures under support excitation", *Eng. Struct.*, **32**(8), 2221-2228.

Lisowski, W. (2003), "An example of model consolidation in autonomous modal analysis (in Polish)", *Problems of Modal Analysis of Mechanical Structures - Collective Work Edited by Tadeusz Uhl*, KRiDM Publisher, AGH, Krakow, Poland.

Manka, M., Rosiek, M., Martowicz, A., Stepinski, T. and Uhl, T. (2013), "Lamb wave transducers made of piezoelectric macro-fiber composite", *Struct. Control Health Monit.*, **20**(8), 1138-1158.

McHargue, P.L. and Richardson, M.H. (1993), "Operating deflection shapes from time versus frequency domain measurements", *Proceedings of the 11th International Modal Analysis Conference*, Orlando FL, February.

Meirovitch, L. and Baruh, H. (1982), "Control of self-adjoin distributed-parameter systems", *J. Guid. Control Dynam.*, **5**(1), 60-66.

Mendrok, K. and Kurowski, P. (2013), "Operational modal filter and its applications", *Arch. Appl. Mech.*, **83**(4), 509-519.

Mendrok, K. and Uhl, T. (2008), "Modal filtration for damage detection and localization", *Proceedings of the 4th EWoSHM*, Krakow, July.

Mendrok, K. and Uhl, T. (2010), "The application of modal filters for damage detection", *Smart Struct. Syst.*, **6**(2), 115-133.

Mendrok, K. and Uhl, T. (2011), "Experimental verification of the damage localization procedure based on modal filtering", *Struct. Health Monit.*, **10**(2), 157-171.

Mendrok, K., Uhl, T. and Bednarz, J. (2009), "Application of modal filtration for damage detection of rotating shaft", *Key Eng.Mater.*, **413**, 373-380.

Pieczonka, L., Aymerich, F., Brozek, G., Szwedo, M., Staszewski, W.J. and Uhl, T. (2013), "Modelling and numerical simulations of vibrothermography for impact damage detection in composites structures", *Struct. Control Health Monit.*, **20**(4), 626-638.

Schwarz, B.J. and Richardson, M.H. (1999), "Introduction to operating deflection shapes", *CSI Reliability Week*, **10**, 121-126.

Slater, G.L. and Shelley, S.J. (1993), "Health monitoring of flexible structures using modal filter concepts", *Proceeding of SPIE*, **1917**, 997-1008.

Uhl, T., Lisowski, W. and Kurowski, P. (2001), *In-operation modal analysis and its applications*, KRiDM Publisher, AGH , Krakow, Poland

Wentzel, H. (2013), "Fatigue test load identification using weighted modal filtering based on stress", *Mech. Syst. Signal Pr.*, **40**(2), 618-627.

Wojcicki, J., Mendrok, K. and Uhl, T. (2013), "Spatial filter for operational deflection shape component filtration", *Key Eng. Mater.*, **569**, 868-875.

Zhang, Y., Lie, S.T. and Xiang, Z. (2013), "Damage detection method based on operating deflection shape curvature extracted from dynamic response of a passing vehicle", *Mech. Syst. Signal Pr.*, **35**(1-2), 238-254

Zhang, Q., Allemang, R.J. and Brown, D.L. (1990), "Modal filter: concept and applications", *Proceedings of the 8th International Modal Analysis Conference*, January.

CC